

# SRL: Scaling Distributed Reinforcement Learning to Over Ten Thousand Cores

Zhiyu Mei\*  
meizy20@mails.tsinghua.edu.cn  
Institute for Interdisciplinary  
Information Science,  
Tsinghua University  
Beijing, China  
Shanghai Qi Zhi Institute  
Shanghai, China

Wei Fu\*  
fuwth17@gmail.com  
Institute for Interdisciplinary  
Information Science,  
Tsinghua University  
Beijing, China  
Shanghai Qi Zhi Institute  
Shanghai, China

Guangju Wang  
wanggj@sqz.ac.cn  
Shanghai Qi Zhi Institute  
Shanghai, China

Huanchen Zhang  
huanchen@tsinghua.edu.cn  
Institute for Interdisciplinary  
Information Science,  
Tsinghua University  
Beijing, China  
Shanghai Qi Zhi Institute  
Shanghai, China

Yi Wu  
jxwuyi@gmail.com  
Institute for Interdisciplinary  
Information Science,  
Tsinghua University  
Beijing, China  
Shanghai Qi Zhi Institute  
Shanghai, China

## ABSTRACT

The ever-growing complexity of reinforcement learning (RL) tasks demands a distributed RL system to efficiently generate and process a massive amount of data to train intelligent agents. However, existing open-source libraries suffer from various limitations, which impede their practical use in challenging scenarios where large-scale training is necessary. While industrial systems from OpenAI and DeepMind have achieved successful large-scale RL training, their system architecture and implementation details remain undisclosed to the community. In this paper, we present a novel system abstraction on the dataflows of RL training, which unifies practical RL training across diverse applications into a general and flexible framework and enables fine-grained system-level optimizations. Following this abstraction, we develop a scalable, efficient, and extensible distributed RL system called Really Scalable RL (SRL). The system architecture of SRL separates major RL computation components and allows massively parallelized training. We also introduce a collection of techniques to further optimize the system performance. Moreover, SRL offers user-friendly and extensible interfaces, which facilitate the development of customized algorithms. Our evaluation shows that SRL outperforms existing academic libraries in both a single machine and a medium-sized cluster. In a large-scale cluster, the novel architecture of SRL leads to up to 3.7x speedup compared to the design choices adopted by the existing libraries. We also conduct a direct benchmark comparison to OpenAI’s industrial system, Rapid [5], in the challenging hide-and-seek environment[2]. SRL reproduces the same solution as reported by OpenAI with up to 5x speedup in wall-clock time. Furthermore, we also examine the performance of SRL in a much harder variant of the hide-and-seek environment and achieve substantial learning speedup by scaling SRL to over 15k CPU cores and 32 A100 GPUs.

\*Equal contribution.

Notably, SRL is the first in the academic community to perform RL experiments at such a large scale.

## 1 INTRODUCTION

Reinforcement Learning (RL) is a prominent subfield of machine learning that trains intelligent decision-making agents to maximize a cumulative reward signal, which has been a popular paradigm leading to a lot of AI breakthroughs, including defeating world champions in various competitive games [5, 29, 34, 39], controlling a tokamak nuclear fusion reactor [8], discovering novel algorithms [13], and creating intelligent robots [23]. In RL, an agent interacts with an environment by taking an *action* based on its current *observation*, and the environment responds by providing a new observation and a scalar *reward* signal. The goal of the agent is to learn a neural network *policy*, which is a mapping from observations to actions, that maximizes the expected cumulative reward over time. An RL algorithm leverages the collected sequence of observations, actions, and rewards (i.e., *trajectories*, *samples*, or *training data*), to optimize the policy parameters via gradient descent.

As RL tasks getting more and more complex, training a strong neural network policy requires millions to billions of trajectories, as we show in Table 1. Simply generating such a massive amount of data sequentially would take hundreds or even thousands of years. Therefore, building a system that can parallelize the data collection process and perform efficient RL training over the massive trajectories becomes a fundamental requirement for applying RL to real-world applications.

**Table 1: Data volume and required CPU time of prior works.**

Agent	Domain	# Env.Frames	# CPU×Time (Year)
DeepMind Agent57 [1]	Atari	$9 \times 10^{10}$	$\approx 9$
OpenAI Five [5]	Dota2	$\approx 1.7 \times 10^{11}$	$\approx 180$
AlphaStar Final [39]	StarCraftII	$\approx 4.6 \times 10^{12}$	$\approx 6000$

Numerous open-source libraries or frameworks are available to facilitate efficient RL training [10, 12, 17, 21, 30, 36, 43, 44]. However, we have identified several limitations in these systems that hinder their abilities to train RL agents efficiently in various scenarios. First, existing open-source systems have made unnecessary assumptions about computing resources, such as types and physical locations of hardware accelerators, making their architectures only efficient in corresponding circumstances. Second, their implementations lack support for multi-node multi-GPU training, which can hinder efficient RL training in complex tasks that require a sophisticated policy and a large batch size. Third, prior works primarily focus on small- to medium-scales, resulting in simplistic implementation details with inadequate considerations for performance optimization. Such limitations render open-source libraries insufficient for supporting large-scale RL training applications like AlphaStar [39] for StarCraft II or OpenAI Five [5] for Dota 2. Unfortunately, the proprietary systems used by OpenAI and DeepMind have not been open-sourced, and the architectural and engineering details have not been extensively shared with the research community. As a result, it remains largely unknown how to develop a system capable of scaling well enough to support RL training in complex environments and maximizing hardware efficiency under available resource constraints.

To address the aforementioned challenges, we present a novel abstraction on the dataflows of RL training. This abstraction effectively unifies training tasks in diverse circumstances into a simple framework. At a high level, we introduce the notion of “*workers*” to represent all computational and data management components, each of which hosts distinct “*task handlers*” such as environments or RL algorithms. Workers are interconnected by “*streams*” and supported by “*services*”. Based on such a framework, we propose a scalable, efficient, and extensible distributed RL system, which we have named SRL (ReaLly Scalable RL), that can be highly efficient in a wide range of scenarios, ranging from local machines to large, customized clusters featuring heterogeneous computation resources. SRL encompasses three primary types of workers: *actor workers* host environment instances, which are responsible for executing environment simulation; *policy workers* host RL agents (or policies), which are responsible for conducting batched policy inference to generate actions; *trainer workers* host RL algorithms, which are responsible for updating policy parameters using trajectories produced by environments. To minimize communication overhead, data transfer between workers is facilitated by *inference streams* and *sample streams*, which can utilize either network sockets or local shared memory. After each training step, updated parameters are pushed to the parameter database and periodically broadcasted to policy workers by the *parameter service*.

The architecture of SRL promotes complete decoupling of workers, thereby allowing for elastic scheduling and finding an optimal configuration on a customized cluster with heterogeneous hardware resources. This flexible approach enables the allocation of specific resources, such as CPUs or GPUs with varying computation powers, based on the requirements of each task handler. Furthermore, SRL is highly adaptable and extensible. In addition to built-in implementations of workers and algorithms that facilitate easy configuration and execution of experiments, SRL provides a general set of APIs that allow users to develop new components that are suitable for

specific use cases. Moreover, through detailed analysis on each type of workers and data streams, we apply a collection of detailed optimizations that improve the overall performance of SRL.

Our experimental evaluation focused on assessing the effectiveness of SRL using two key metrics: *training throughput* and *learning performance*, across various sets of RL environments. The *training throughput* metric measures the rate at which a system can process sample frames per second for gradient updates. We conducted evaluations on a diverse range of academic environments, comparing SRL to various open-source libraries. The results demonstrated that SRL achieved a substantial performance improvement, reaching a maximum of 21.6 times higher performance in a medium-size cluster (with 8 A100 GPUs and 3200 CPU cores) compared to current open-source solutions. In a local single-machine setting, SRL performs on par or even better than state-of-the-art systems specifically designed for this scenario. Additionally, we evaluated the performance of our novel architecture against existing designs in a large-scale cluster (with 32 A100 GPUs, 64 RTX3090 GPUs, and 12800 CPU cores) by implementing them within SRL for a fair comparison. SRL is at least as good as the best previous design and outperforms all previous designs in half of the environments considered. The second metric, *learning performance*, measures the wall-clock time required to train an optimal RL agent. We conducted a benchmark study on the challenging hide-and-seek environment (HnS)[2] by comparing SRL against OpenAI’s industrial production system *Rapid* [5]. In this benchmark, SRL is able to reproduce the same solution quality as *Rapid* while achieving a 3x speedup with CPU inference and a 5x speedup with GPU inference. To further explore the scaling capabilities of SRL, we introduced a more challenging variant of the original hide-and-seek problem [2] by doubling the playground size. Remarkably, SRL successfully solved the more difficult problem with over 15K CPU cores. The training process gets substantially accelerated with an increasing amount of computation. This highlights the exceptional scalability of SRL and underscores the importance of employing large-scale RL training for the most difficult problems. Finally, we conducted extensive ablation studies on SRL and provided guidelines for the optimal system configuration for practical RL training.

The contributions of this work are summarized as follows. First, we provide a novel abstraction on RL dataflows, which can assist in analyzing bottlenecks of existing RL systems and designing flexible APIs for new systems. Second, based on this abstraction, we develop SRL, a scalable, efficient, and extensible distributed RL system that can achieve high training throughput on a local machine while also exhibiting strong scalability in a large cluster. Third, we perform an extensive evaluation of the performance of SRL across a wide range of RL testbeds. SRL shows superior scalability and efficiency compared with existing academic libraries as well as OpenAI’s industrial system. Finally, we perform ablation studies and provide practical guidelines for the community.

## 2 BACKGROUND

### 2.1 Reinforcement Learning

Reinforcement learning (RL) develops algorithms and agents that can learn from interactions with an environment. In RL, an agent

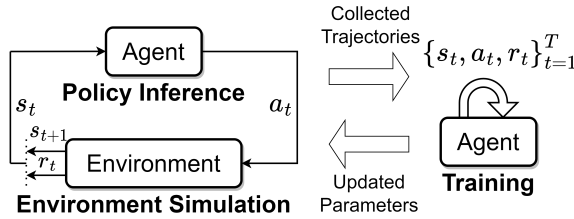


Figure 1: Vanilla implementation of reinforcement learning.

interacts with an environment in discrete time steps with a maximum horizon  $T$ , where it observes the current state  $s_t \in \mathcal{S}$  of the environment and selects an action  $a_t \in \mathcal{A}$  to perform. The environment then transitions to a new state  $s_{t+1} \in \mathcal{S}$ , and the agent receives a reward signal  $r_t \in \mathbb{R}$  and the new observation. Given trajectories  $\{(s_t, a_t, r_t)\}_{t=1}^T$ , the goal is to learn the optimal policy  $\pi : \mathcal{S} \rightarrow \Delta(\mathcal{A})$  that maximizes its cumulative reward over time, i.e.,  $\mathbb{E}_\pi [\sum_{t=1}^T r_t]$ .

As an example, in the game of Go [34],  $s_t$  represents the current board configuration, including the positions of all stones and whose turn it is to play.  $a_t$  refers to the decision about where to place a stone on the board and  $r_t$  refers to the outcome of the game,  $+1/-1$  for a win/loss at timestep  $T$  and 0 otherwise.

In this paper, we focus on designing a distributed system for deep reinforcement learning (DRL), where the policy is represented as a deep neural network that takes the raw sensory input (e.g. images) and produces a probability distribution over possible actions. At each training step, the neural network is optimized using RL algorithms with stochastic gradient descent over collected trajectories. This routine continues until the budget of environment interactions is reached. For ease of reference, we use the term ‘‘RL’’ throughout this paper to refer to deep reinforcement learning.

## 2.2 Reinforcement Learning System

In an RL training process, we identify three major computation components.

- (1) **Environment simulation** produces observations and rewards based on actions. This computation is typically performed using external black-box programs, such as games or physics engines, and is usually executed on CPUs.
- (2) **Policy inference** produces actions from observations, which is conducted by inference (a.k.a. forward propagation) of neural network policies. The system can use either CPU or GPU devices for policy inference, although there can be a clear performance advantage when adopting GPUs [10].
- (3) **Training** executes gradient descent iterations on GPU using the collected trajectories to improve the policy.

Vanilla RL implementations tightly couple the above computations, as shown in Fig. 1: at each training iteration, it first alternatively conducts environment simulation and policy inference to collect trajectories, and then performs training with these data. To improve training throughput, a common practice adopted by the community is to launch multiple environment instances for batched simulation and policy inference. This vanilla implementation is far from efficient because only one of the major computations can be done at the same time.

To train intelligent agents that are able to perform specific tasks with the capability of surpassing human specialists [1, 5, 39], it is crucial to have extremely large volumes of environment interaction steps to derive a sufficiently strong neural policy. Without the help of an efficient system, it is impossible to complete such a training job within a reasonable amount of time. Therefore, extending RL to distributed settings and improving the efficiency represents a vital research direction.

The primary goal of designing an RL system is to efficiently utilize available hardware resources (local machine or a cluster) to improve RL training throughput. It requires that (1) training samples (trajectories) are generated quickly, and (2) trainers consume samples in a speed that keeps up with the sample generation. Besides the major computation components, designers should take additional care of data transmission, data storage, and parameter synchronization.

## 2.3 Motivation

There are many existing open-source RL systems that offer solutions for specific application scenarios [6, 7, 14, 15, 17, 21, 28, 30, 35, 36, 43, 44]. However, only a few of them are general-purposed, namely RLLib [21], ACME [17], SeedRL [10], Rlpyt [36], and Sample Factory [30]. However, based on our research and evaluation, we have found that these libraries have their limitations in both architecture designs and implementations.

*First, regarding architecture design, most of the open-source libraries have made assumptions in available computation resources, such as types and physical locations of hardware accelerators, and ratio between available computational devices. Consequently, their architectures tend to tightly couple multiple computational components and map them onto devices that are physically located on the same node, which can be detrimental to system performance when deployed in customized local clusters.*

Specifically, Sample Factory [30] and Rlpyt [36] are specifically for RL training in a local machine and do not assume distributed computation resources are available. Other libraries that take distributed settings into considerations could usually be classified into two types: IMPALA-style [11] and SEED-style [10].

The IMPALA-style architecture, represented by RLLib and ACME (Fig. 2 top), assumes a tight coupling between the computational resources used for environment simulation and policy inference. In this setup, policy inference can only be performed on CPUs or GPUs that are located on the same node as the environments. While using CPUs for policy model inference is inherently inefficient, using local GPUs for inference also has critical drawbacks. Depending on the application scenario, the variation of environment simulation speed, observation size, and policy model size may easily cause idle or overloaded inference on the local GPU and lead to significant resource waste. Additionally, if agents follow different policies in multi-agent environments, the local GPU must maintain multiple policy models, leading to significant memory usage and constraining the number of environments that this node can accommodate.

The SEED-style architecture (Fig. 2 down) primarily assumes separate TPU cores are available for training and policy inference.

**Table 2: Capabilities of open-source RL system implementations.**

	Distributed Execution	Multi-Node Training	Remote GPU Inf.	Custom RL Algo.	Custom DataFlow
RLlib [21]	✓	✗	✗	✓	✗
SampleFact. [30]	✗	✗	✗	✗	✗
rlypt [36]	✗	✗	✗	✗	✗
SeedRL [10]	✓	✗	✓	✗	✗
ACME [17]	✓	✗	✗	✓	✗
MSRL [44]	✓	✗	✗	✓	✓
SRL (ours)	✓	✓	✓	✓	✓

✓: Limited support that follows restricted architectures or APIs.

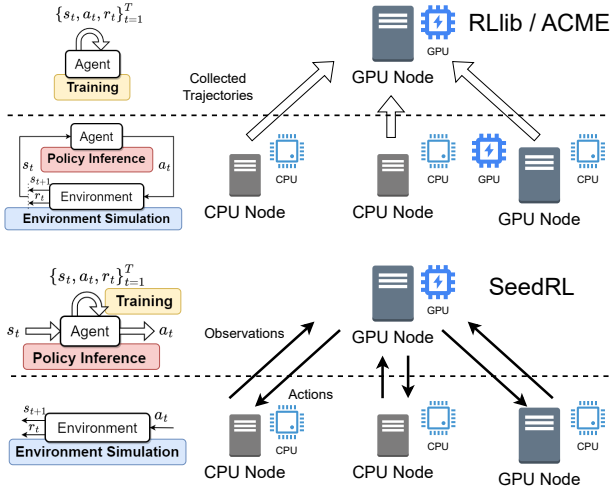


**Figure 2: Implementations of RLLib/ACME (top) and SeedRL (down), following IMPALA-/SEED-style architectures. The former merges environment simulation and policy inference in a single thread, while the latter merges policy inference and training on a single GPU. Note that in SEED-style, GPU nodes running environment simulation rely on the training GPU node for policy inference, while in IMPALA-style, they rely on local CPU/GPU for policy inference.**

However, in the case of GPUs instead of a multi-core TPU, it can struggle to handle both inference and training. Furthermore, training throughput will be limited by stragglers in gradient synchronization when using heterogeneous GPUs.

Second, considering implementation, open-sourced distributed systems do not scale training across multiple nodes, which can hinder RL training in complex tasks that require a sophisticated policy and a large batch size [2]. Specifically, RLLib and ACME only support local multi-GPU training via Python threaded trainer<sup>1</sup> and `jax.pmap`<sup>2</sup>, respectively, while SeedRL can only run on a single GPU.

Third, open-source libraries primarily focus on small to medium scales, resulting in simplified implementations with limited considerations for fine-grained performance optimizations. Consequently, these systems lead to poor training throughput, especially in large-scale scenarios. Through an analysis of their design and implementation, we have identified several possible optimizations that are capable of significantly enhancing system performance. Applying

these modifications yields a noteworthy enhancement in training throughput, which helps SRL outperform pre-existing systems by a considerable margin.

Moreover, despite some existing open-source libraries providing a general interface that allows for customized environments and RL algorithms for users (e.g. RLLib), their algorithm implementation is closely intertwined with their system APIs. These systems lack a user-friendly interface that enables the expansion of system components, which restricts their compatibility with complex RL algorithms (such as MuZero [32]) that require computations beyond the three major RL computation components mentioned in Sec. 2.2.

There have been concurrent efforts that aim to address these limitations. MSRL [44] adopts a compilation approach, which transforms user code that runs locally into “fragments” divided by a set of “annotations” that mark the boundaries and define the dataflow. These fragments could be executed in a distributed cluster following pre-defined scheduling plans. However, compared with SRL, this approach has its drawbacks. First, the computation and communication APIs that can be compiled by MSRL are highly restricted. This set of APIs could only support classic RL algorithms (e.g. DQN and PPO) while cannot be extended by users. Second, MSRL does not consider system-level computation optimizations in its implementation, leading to much lower training efficiency. Third, when dissecting user-side implementation into executable “fragments”, MSRL follows a set of pre-determined scheduling plans. However, these scheduling plans still follow the existing architectures (i.e., IMPALA-/SEED-style), which are only sufficient for specific RL applications.

To conclude, Table 2 presents the capabilities of previous and concurrent works compared to SRL. To the best of our knowledge, SRL is the first academic system that provides all the desired properties, including scalability, efficiency and extensibility. The remainder of this paper is structured as follows: Sec. 3 presents a detailed introduction of SRL’s architecture and provides a justification for the chosen design. Sec. 4 highlights some performance optimizations employed in the system. Sec. 5 outlines the experiment methodology and presents the results. Sec. 6 introduces related works to this paper. Finally, Sec. 7 concludes the paper.

## 3 SYSTEM ARCHITECTURE

### 3.1 High-Level Design of SRL

To address the limitations of previous designs, we propose a novel abstraction on the dataflows of RL training. In the abstraction, SRL is composed of multiple interconnected “workers” that host distinct “task handlers”, such as environments and RL algorithms. These workers are connected via data “streams” and supported by background “services”. Base on this simple abstraction, we develop the architecture of SRL as illustrated in Fig. 3. SRL incorporates three core types of workers: *actor worker*, *policy worker*, and *trainer worker*, which are responsible for the three pivotal workloads in RL training tasks introduced in Sec. 2. Actor workers simulate environments – they produce rewards and next-step observations based on received actions. Policy workers perform batched forward propagation of the neural policy to generate actions given observations. Trainer workers run stochastic gradient descent steps given training samples to update the policy. Actor workers post inference requests containing

<sup>1</sup>[https://github.com/ray-project/ray/blob/master/rllib/execution/multi\\_gpu\\_learner\\_thread.py](https://github.com/ray-project/ray/blob/master/rllib/execution/multi_gpu_learner_thread.py)

<sup>2</sup><https://github.com/deepmind/acme/blob/master/acme/agents/jax/ppo/learning.py#L393>

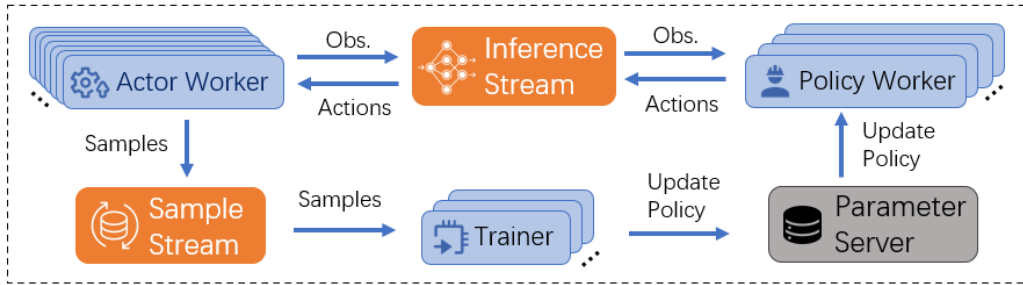


Figure 3: Core components of SRL. Blue arrows show dataflow between workers and data streams. Blue boxes represent workers, which are responsible for computational workloads. Orange boxes represent data streams, which are responsible for communication between workers. The grey box represents service, which is the parameter server in our context.

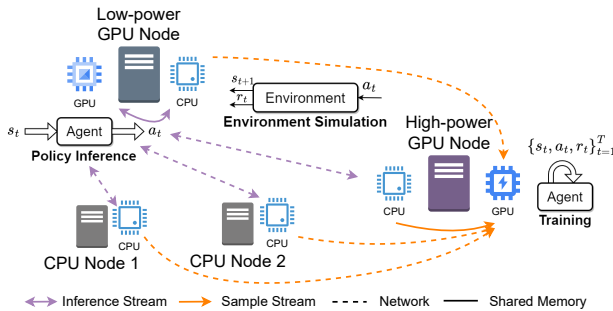


Figure 4: Distributed workload of SRL that can fully utilize all heterogeneous computation resources.

observations to policy workers, and policy workers respond by the generated actions. We abstract this client-server communication pattern as *inference stream*. In parallel with environment simulation, actor workers accumulate observation-action-reward tuples in the local buffer and periodically sends them to trainer workers. We abstract this push-pull communication pattern as *sample stream*. After each training step, the updated parameter is pushed to a *parameter server*, which handles pull requests from policy workers for parameter synchronization.

Unlike previous designs, all workers in SRL can be independently scheduled and distributed across multiple machines with heterogeneous resources, allowing for massive parallelism and efficient resource utilization under various resource settings, including both local machines and large clusters. As depicted in Figure 4, we have instantiated the abstracted workers as processes on different computing nodes, and data streams as sockets or shared memory blocks. Each worker is assigned with a specific amount of computing resources that suits its task, and workers are connected via the most efficient interface available, which can be networking for inter-node communication or shared memory for inter-process communication. As a result, the novel architecture of SRL not only unifies existing local and distributed architectures with a clear design and implementation, but also enables efficient scheduling, resource allocation, and data communication for scenarios beyond the capabilities of existing architectures. Moreover, the clear design of SRL enables fine-grained performance optimization, resulting

in significant improvements in speed and scalability compared to existing libraries, even when using the same architecture. Furthermore, the high-level abstraction produces a clean user interface, making it effortless to extend existing RL algorithms and customize workers.

In Sec. 3.2, we will provide a detailed description of each system component and explain how SRL attains scalability and efficiency as an integrated system. In Sec. 3.3, we will introduce the user-friendly and extensible designs interfaces of SRL with practical examples.

## 3.2 System Components

We remark that the following content assumes a typical workflow of most popular RL algorithms (e.g., PPO [33] or DQN [25]) for a clear presentation. There do exist RL algorithms (e.g., MuZero [32]) requiring a more complicated system design, which will be discussed later in Sec. 3.3 without confusing readers herein. These unusual algorithms can be also supported by SRL easily.

**3.2.1 Actor worker and Policy worker.** Actor workers host environments to handle the execution of black-box environment programs. Environment simulation is usually self-contained within each actor, making it straightforward to be massively parallelized given sufficient computation resources. On the other side, policy workers host RL agents (or policies) and provide batched inference service for actor workers. They can effectively utilize GPU devices for accelerated neural policy forward propagation.

Environment simulation is usually divided into episodes. In the beginning of each episode, an actor worker resets its environment and gets the first observation. Then before every environment step, each actor worker sends out the observation of the last step (or the initial reset) and requests an action from policy workers to continue to the next step. Actor workers are inherently designed to be multi-agent, such that (1) different actor workers can host different number of agents, (2) agents can asynchronously step through the environment (skip if the environment returns None), and (3) agents can apply different policies by connecting to different streams. This flexible design enables SRL to deal with more complex and realistic application scenarios (see examples in Sec. 3.3).

Policy workers flush received inference requests from multiple actor workers, compute forward passes on policy models with batched observations, and respond them with output actions. To

**Table 3: Model size in RL versus supervised learning.**

Domain	Atari DQN [25]	Robot Control [33]	Vision (ResNet18 [16])	Language (Transformer [38])
Type	convolution	feed-forward	convolution	attention
# Params	3.29M	< 1M	11M	65M

keep policy models up-to-date, policy workers also need to pull parameters from parameter servers once in a while. Data transmission, parameter synchronization, and neural network inference are handled in three different threads.

We remark that there do exist circumstances, such as no GPU devices available or very limited network bandwidth, where launching policy workers on separate machines may not be preferred. Our implementation of policy worker also supports a local CPU mode, which we call *inline inference*. In this case, inference stream module will ensure direct data transmission between an actor and its associated local policy worker with proper batching and without using the network. Although our inline inference mode is conceptually similar to RLlib and ACME, the implementation of actor worker and policy worker remains unchanged with different hardware supports, leading to enhanced flexibility for practical use.

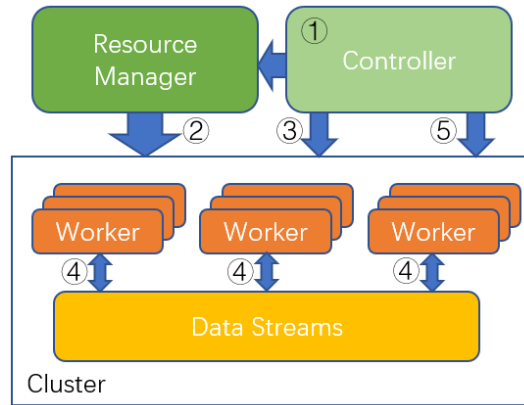
**3.2.2 Trainer workers.** Trainer workers are responsible for computing gradient descent iterations. They receive samples from actor workers. Each trainer worker is embedded with a buffer to store samples waiting for being fetched into GPU. Before every iteration of gradient descent, a trainer worker aggregates a batch of samples from data buffer and load them into its GPU device. Jobs on CPU and GPU are separated into two threads.

In SRL, we support multi-GPU training across nodes. By our multi-trainer design, each trainer worker is assigned to exactly one GPU device, which means one trainer worker is a minimal unit for training computations.

Note that policy models in RL are usually small in size (see Table 3), so model parallelization is not required in most applications. Hence, we adopt single-program multi-data (SPMD) paradigm for our multi-trainer design. For a large batch of samples, we evenly distribute samples to multiple trainers, every one of which holds a copy of the same policy model. Each trainer computes gradient using their own copy, and synchronize the gradients to update the final policy model at the end of every training iteration. Trainer workers use PyTorch DistributedDataParallel (DDP) [20] as the backend that communicate trainers and synchronize the gradients.

Additionally, there are circumstances where a single trainer worker may not be able to fully utilize the computing power of a GPU. To prevent unnecessary waste of computing powers, we allow other workers (e.g. policy workers) to share one GPU with a trainer worker.

**3.2.3 Sample streams and Inference streams.** In SRL, we identify two primitive types of data transmissions between workers. One is exchanging observations and actions between actor workers and policy workers. The other is sending samples from actor workers to trainer workers. Corresponding to the two types of data transmissions, we develop inference streams and sample streams, which have different data transmission patterns. Inference streams need to be duplex because actor workers send inference requests and

**Figure 5: Running an experiment with SRL on a cluster. Numbers in a circle represent steps in this procedure.**

policy workers are required to reply. Meanwhile, sample streams are simplex. Only actor workers send training samples to trainer workers, and trainer workers do not reply.

For network transfer, we implement inference stream as a pair of request-replay sockets and sample stream as a pair of push-pull sockets. For local shared-memory transfer, we instantiate inference stream as a block of pinned shared memory, i.e., each client is assigned to exactly one slot for read and write, and sample stream as a well-designed shared-memory FIFO queue.

We also discuss some special use cases of data stream. In certain RL applications, such as multi-agent RL and population-based training, multiple policy models need to be trained in one training experiment. This suggests that different actor workers need to communicate with a specific groups of policy workers and trainer workers holding certain policy models. Therefore, multiple instances of sample streams and inference streams in one experiment can be required. Different data streams establish independent and perhaps overlapped communications between groups of workers to ensure data from different policies never contaminate each other.

**3.2.4 Parameter server.** In RL training, policy models used in training and policy inference need to be synchronized regularly. In SRL, parameter server is the intermediate station for policy models. After a certain period of time, trainer workers will push a newer version of policy models to parameter server. Policy workers check version of their policy model in parameter server once in a while. If parameter server stores a newer version, policy workers will pull the model immediately. Since most of policy models in RL applications are not large in size compared with supervised learning (see Table 3), parameter server is usually not the bottleneck of SRL. We provide two implementations of parameter server, one based on NFS, and the other one running a background serving thread which broadcasts updated parameters to each node for the query of policy workers. The NFS variant has enough throughput for common usage according to our experience, which we therefore apply for all experiments.

**3.2.5 Controller.** In SRL, an experiment denotes a complete RL training task, which needs to be run on a large-scale cluster with

```

class MyDQNPolicy:
    def __init__(self, **kwargs):
        # Can be feed-forward, recurrent, convolution,
        # or even tree-search policies.
        self.net = MyNet(**kwargs)
        ...
    def rollout(self, request: Dict[Tensor]):
        # This method is used by policy workers.
        self.net.eval()
        q, policy_state = self.net(request['obs'],
            request['policy_state'])
        ... # Can do tree-search here.
        act = eps_greedy_select(q)
        return {'action': act,
            'policy_state': policy_state}
    def analyze(self, sample: Dict[Tensor]):
        # This method is used by the RL algorithm.
        ...

class MyDQNAlgorithm:
    def __init__(self, policy: MyDQNPolicy, **kwargs):
        ... # Store algorithm hyper-parameters.
        # The API called by trainer workers.
    def step(self, sample: Dict[Tensor]):
        q, q_target = self.policy.analyze(sample)
        loss = mse_loss(q, q_target)
        ... # Gradient descent step.
        self.policy.inc_version()
        return {'loss': float(loss)}

```

**Code 1: Python example of a simplified deep Q-learning. Users can write new neural network models and RL algorithms without knowing any system related APIs.**

multiple nodes. Figure 5 shows steps to run an experiment on a cluster using SRL. We dissect an entire run of experiment into following 5 steps:

- (1) Launching controller with experiment configurations and apply resources.
- (2) Allocate resources with resource manager.
- (3) Launching and configuring workers with controller.
- (4) Workers connect to data streams and run tasks.
- (5) After finishing experiment, stop workers.

In this procedure, a pivotal component is controller. It allocate resources from resource manager, handles experiment configurations and manages the life cycle of workers and data streams. Its implementation has two parts. The first one is a client to resource manager service (we use `slurm` [42] as our resource manager in the cluster). The second one is an RPC client that launches workers (as RPC servers) and send requests to workers.

### 3.3 User-friendly and Extensible Designs

In addition to its high scalability and efficiency, SRL offers user-friendly and extensible interfaces, allowing for the development and execution of customized environments, policies, algorithms, and architectures within its framework.

Previous works have presented systems or libraries that support customization under fixed system architectures, such as `RLlib` [21] and `ACME` [17]. For example, users can create new neural policies or RL losses under their framework. However, their implementation, particularly RL algorithms, is closely linked to system APIs. This means that, for instance, users are required to adhere to the use of the `RolloutWorker` API in `RLlib` or the `reverb` library

```

ExperimentConfig(
    actors=[
        ActorWorker(
            env="remote_reward_compute_env",
            inference_streams=["pol_inf", "rwd_inf"],
            sample_streams=["rl_train", "null_stream"],
            agent_specs=[
                AgentSpec(
                    index_regex="0", # the first agent
                    # matches to the first inf stream
                    inference_stream_idx=0,
                    sample_stream_idx=0,
                ),
                AgentSpec(
                    index_regex="1",
                    inference_stream_idx=1,
                    sample_stream_idx=1,
                )
            ],
        ) for _ in range(128)
    ],
    policies=[PolicyWorker(
        inference_stream="pol_inf",
        policy="rl_policy",
    ) for _ in range(4)] +
    [PolicyWorker(
        inference_stream="rwd_inf",
        policy="clip", # The large pretrained model.
    ) for _ in range(1)],
    trainers=[TrainerWorker(
        trainer="ppo",
        policy="rl_policy",
        sample_stream="rl_train",
    )],
)

```

**Code 2: Example configuration for computing rewards in remote policy workers hosting large pre-trained models.**

with `ACME` to manage training data in a customized algorithm, hindering convenient development. In contrast, policies and algorithms in SRL are separated from system design, allowing users to develop new variants without using any system-related interfaces. We demonstrate a concrete example in Code 1. To implement Deep Q-Network [25], users only need to write a policy file that defines the policy’s behavior during data collection and training, and an algorithm file that specifies how to compute the scalar loss given data obtained from the policy. These files can be entirely independent of existing algorithm implementations and system APIs, which enables users to focus on algorithm development rather than being distracted by the heavy system code.

Additionally, SRL offers versatile configuration options and a generic interface for both new workers and data streams, facilitating complete customization of dataflow and algorithmic modules. We present two practical examples in Code 2 and Code 3. The first instance depicts a scenario where rewards returned by the environment must be computed using a pre-trained (large) neural network model rather than the program itself. With SRL, users can create an additional sentinel agent for reward computation. This agent is linked another inference stream and policy worker, which host the reward model. After each environment step, real agents return `None` and the sentinel agent issues a reward computation inference request. After the reward is returned, the sentinel agent returns `None` and real agents return next-step observations and computed

```

class Worker:
    def __init__(self, server):
        server.register('configure', self.configure)
        ... # Other RPCs for starting, exiting, etc.
    def configure(self, config):
        r = self._configure(config)
        ...
        self.__worker_type = r.worker_type
        self.__worker_index = r.worker_index
    def run(self):
        while not self.__exiting:
            r = self._poll()
            ... # Deal with poll results.
            self._server.handle_requests()
class BufferWorker(Worker):
    def _configure(self, cfg: api.config.BufferWorker):
        ... # Init streams and the augmentor.
        r = cfg.worker_info
        return r
    def _poll(self):
        # Connected with actor worker.
        x, cnt = self.up_spl_stream.consume_to(self.buf)
        # The "task handler".
        y = self.augmentor.process(self.buf.get())
        # Connected with trainer worker.
        self.down_spl_stream.post(y)
        return PollResult(sample_count=cnt, batch_count=1)

```

**Code 3: Worker API in SRL and the implementation of a customized buffer worker for data re-processing.**

reward to advance environment simulation. In the second example, SRL enables the implementation of an additional computation module that supports periodic reprocessing of previously generated samples, known as “re-analyze” in the MuZero algorithm [32]. Although this module does not fit into the primary computation components depicted in Fig. 1, users can easily create a self-defined

`BufferWorker` by inheriting the base `Worker` class and overwriting worker’s execution step to perform such computation. This worker-based customization further facilitates the development of complex RL training routines within our framework.

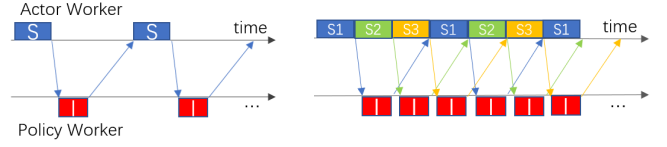
## 4 PERFORMANCE OPTIMIZATIONS

In this section, we will introduce optimization techniques that contributes to the overall performance of SRL.

### 4.1 Trainer Data Pre-fetching

A typical working cycle for a trainer worker consists of three steps: storing received data in the buffer, loading data into GPU and computing gradient for model update. The first two steps, receiving and loading data, are I/O heavy operations. Overlapping these steps with the third step can lead to higher sample throughput than executing them sequentially on a trainer worker. While receiving and storing data into buffer could be simply implemented into a separate thread, model update on a sample batch requires data loading as a dependency. To overlap computing the gradient for model update with data loading, we use a data pre-fetching technique.

To implement this technique, we reserve GPU memory for two batches of training samples. When training starts, one sample batch is fetched into GPU memory. Then, while the GPU computes the gradient on this sample batch, another sample batch is pre-fetched into the other memory block simultaneously. In this way, all three steps



(a) Timeline for a trivial actor worker with one environment instance.

(b) Timeline for an SRL actor with environment ring of size three (3 environment instances).

**Figure 6: Comparison between a trivial actor and an actor with environment ring. A box labelled with “S” represent environment interaction step, and different colors denote different instances. A red box labelled with “I” represent an inference step. Arrows between timelines are observations and actions transmitted between actor worker and policy worker.**

in the trainer working cycle will be executed in parallel threads, which further improves SRL’s training performance.

### 4.2 Environment Rings

In actor workers, environment simulation usually follows a two-stage loop: an actor simulate a black-box program by feeding in an action to receive an observation, and then wait until an action is received from the policy worker. In this process, the CPU will be periodically idle when the action is being processed by the policy worker (Fig. 6a). To fully utilize the CPU resources, an actor in SRL maintain multiple environment instances and execute each environment instance sequentially. We call this technique an *environment ring*. With an environment ring, when an environment instance finishes simulation and starts waiting for an action, the actor will immediately switch to the next environment instance. With a proper ring size, we can ensure that when simulating an environment instance, the required action is always ready (Fig. 6b). Environment rings substantially eliminate idle time for actors, and thus greatly increase data generation efficiency for actor workers. The optimal ring size usually depends on the speed of environment simulation, observation size, and policy model size.

## 5 EXPERIMENTS

In this section, we present an empirical evaluation of our system, focusing on two key metrics: *training throughput* and *learning performance*. Training throughput refers to the rate at which a system can process sample frames per second for gradient updates, while learning performance measures the wall-clock time required to generate the optimal solution.

To assess the training throughput of SRL, we conduct experiments in both single-machine and distributed settings. We compare the performance of SRL against existing open-source libraries using a selection of well-known academic testbeds. Additionally, we evaluate the efficiency of our novel RL architecture by comparing its throughput to two existing architectures, as described in Section 2.3, in a large-scale cluster.

To evaluate the learning performance of SRL, we choose a much more challenging hide-and-seek environment [2] and examine the required training time to reproduce the same solution quality as OpenAI’s industrial system, Rapid [5]. We remark that the academic

**Table 4: Characteristics of adopted environments.**

	Atari (Pong)	Deepmind Lab (watermaze)	gFootball (11_vs_11)	SMAC (27m_vs_30m)
Observation	Image	Image	Vector	Vector
# Controlled Agents	1	1	22	27
Third-Party Engine	No	No	Yes	Yes
Background Process	No	No	No	Yes
Pure Simulation FPS	4800	300	75	35
Memory (MBytes)	~100	~250	~170	~1500

testbeds are not chosen here since they are too simple in our computation scale. It is also worth noting that the optimal solution to the hide-and-seek environment necessitates a substantial number of training samples and has never been produced by any existing academic RL systems. To further explore the scaling capabilities of SRL and validate the benefits of large-scale RL training, we even evaluate SRL in a much harder variant of the problem by doubling the size of the hide-and-seek playground.

Finally, we conduct a comprehensive series of ablation studies on various components of our system. These studies allow us to gain insights into the effects of different system configurations and provide practical recommendations for optimizing the performance of SRL in diverse circumstances.

As for RL algorithms, we employ Proximal Policy Optimization (PPO) [33] as our primary choice. PPO is an on-policy algorithm that requires fresh trajectories generated by a recent policy and utilizes a FIFO queue to receive and process training data. In contrast, off-policy algorithms like Deep Q-Network [25] rely on a large replay buffer to store historical trajectories and fetch data from it for training. We remark that on-policy methods are preferable for evaluating training throughput, as training speed is closely related to sample generation speed. It is noteworthy that on-policy algorithms have a similar workload on the trainer worker side. Although other on-policy RL algorithms such as IMPALA [11] are also valid, we have chosen PPO as it is a highly popular RL algorithm for large-scale training and has demonstrated success in various RL applications [2, 5, 41].

Experiments are evaluated on two resource settings<sup>3</sup>:

- (1) Local single-machine setting: 32 physical CPU cores, 512GB DRAM and an Nvidia 3090 GPU.
- (2) Distributed cluster setting: 4 nodes with 64 physical CPU cores and 8 Nvidia A100 GPUs + 64 nodes with 128 physical CPU cores and an Nvidia 3090 GPU. Each node in the cluster had 512GB DRAM and are connected to each other by 100 Gbps intra-cluster network. Storage for the cluster was facilitated through NFS and parameter service, available on all nodes.

## 5.1 Training Throughput

We compared performance of SRL with baselines on both local and distributed settings. The metric we use for evaluation is training environment frames per second (FPS), which refers to the number of environment frames consumed by all trainer workers per second.

<sup>3</sup>All physical cores have hyperthreading enabled and count as 2 logical cores. In this section, if not emphasized, the term “CPU cores” will be referring to logical CPU cores.

Across all experiments in this section, we follow a pure online RL setting: each generated trajectory will be trained only once without reuse. When comparing to baselines, we have made our best efforts to ensure that the experiment configurations are always consistent for all the systems, such as the policy model architecture, algorithm hyper-parameters (e.g. batch size), and the number of processes (CPU cores) running environment simulation.

**5.1.1 Environments.** We run experiments on a set of academic environments, including Atari 2600 games (Atari) [4] (game *Pong*), Google Research Football (gFootball) [18] (scenario *11\_vs\_11*), StarCraft Multi-Agent Challenge (SMAC) [31] (map *27m\_vs\_30m*), and Deepmind Lab [3] (scenario *watermaze*), each of which possesses distinct characteristics in terms of observation type, speed, memory, etc (see Table 4). In Atari and DMLab environments, we adopt a traditional 4-frameskip setting, meaning that number of environment frames is 4 times actual training sample steps.

**5.1.2 Comparison with Baselines.** In the single-machine setting, we choose Sample Factory [30], rlpyt [36], and SeedRL [10] as our baselines. Sample factory and rlpyt are both specialized systems only optimized for single-machine scenarios. SeedRL was originally designed for TPU training in distributed settings. However, even samples generated in one machine can easily overburden its single “learner”. Therefore, we only evaluated SeedRL in the single-machine setting. Fig. 7 shows that, SRL has a superior performance on Atari, achieving almost 30% acceleration compared to Sample Factory, which has the best performance among baselines. In other environments, SRL performs similarly or slightly better compared to Sample Factory. As for MSRL [44], we evaluated against its performance described in paper <sup>4</sup>. The result shows that our system could reach 2.52x training FPS compared to MSRL under the same experiment settings. From the results, we demonstrate that SRL is capable of achieving competitive performance in the single-machine setting against state-of-the-art systems specialized for this scenario without sacrificing its scalability and flexibility.

We also conducted an experiment to evaluate the distributed training capabilities of SRL in comparison to RLlib [21]. While ACME [17] shares a similar architecture as RLlib, we found that the reported number of training throughput in its technical paper [17] is several times lower than RLlib in the same setting. The reported number also matches the results of our early experiment. Hence, we choose RLlib as our baseline in the distributed scenario. In this experiment, We utilized 8 Nvidia A100 GPUs as trainer devices on the same machine with actors across different machines. For RLlib, we gradually increased the number of CPU cores until the trainers were fully occupied, and adding more CPU cores would not increase the overall throughput. We then record the number of CPU cores used and run the same configuration for SRL. Further, we also evaluated the highest FPS number that SRL is capable of reaching with 8 trainer workers. The results, presented in Table 5, demonstrate that SRL achieved 6.3x to 21.6x higher maximal performance, and 1.4x to 3.3x performance when using the same

<sup>4</sup> Sec. 7.3 Fig. 9(a) in [44]: PPO with 320 Mujoco Halfcheetah environments and 24 Nvidia V100 GPUs for inference, MSRL can finish one episode of 1000 steps in 3.85s, FPS 83116. SRL uses same numbers of CPU cores and 4 Nvidia 3090 GPUs for inference, trainer throughput FPS 210165. Experiment details obtained via direct correspondence with authors.

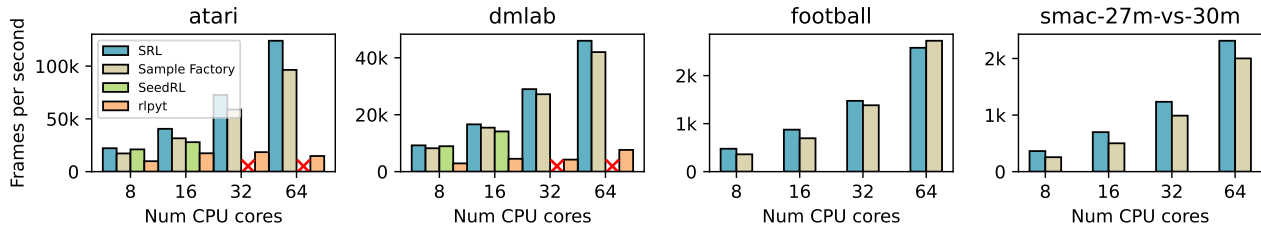


Figure 7: Training FPS of SRL and baselines on a single machine with up to 64 actor CPU cores. SeedRL with 32 and 64 actor CPU cores results in GPU out-of-memory. SeedRL and Rlpyt do not support multi-agent environments, hence can only be evaluated on Atari and DMLab.

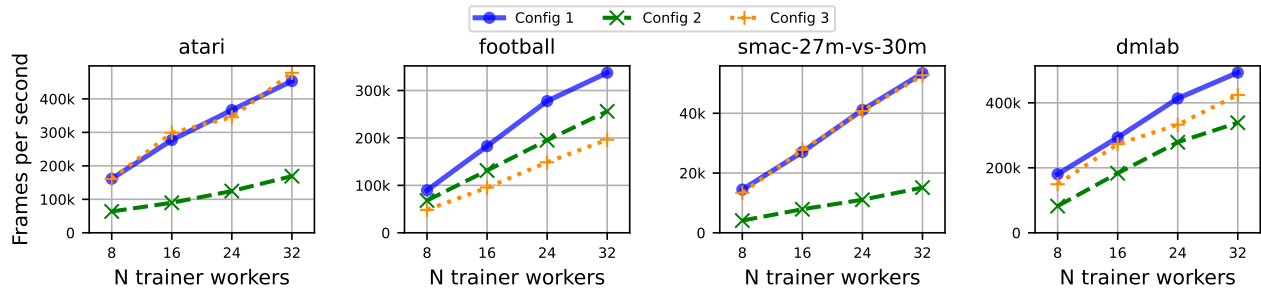


Figure 8: Training FPS of SRL with three different configurations in a large-scale cluster, using up to 32 Nvidia A100 GPU, 32 Nvidia GeForce RTX 3090 GPU and 12800 CPU cores. Config 1: Decoupled workers. Each trainer worker has one A100 GPU and 4 policy workers share one RTX 3090 GPU. Config 2: Coupled trainer worker and policy worker. One trainer worker and 4 policy workers share one A100 GPU. Config 3: Coupled actor worker and policy worker (inline inference). Trainer worker has one A100 GPU. Inference is done on CPU cores.

Table 5: Training throughput of SRL and RLib with 8 A100 GPU trainers. # CPU Cores (peak): CPU cores used for training sample generation when trainers reaches peak performance.

	Atari	Deepmind Lab	gFootball	SMAC
SRL(FPS)	643916	741396	89132	17053
# CPU Cores (Peak)	800	1600	3200	1280
SRL(FPS)	150288	65768	18988	4943
# CPU Cores	96	160	700	200
RLlib(FPS)	65585	34274	5802	2713
# CPU Cores (Peak)	96	160	700	200

numbers of CPU cores compared to RLib. We remark that trainer workers of SRL can effectively utilize training samples generated by much more CPU cores compared to RLib’s single-endpoint multi-threaded trainer. Moreover, actor workers in SRL are capable of generating more training samples with GPU-accelerated inference and environment rings. As a result, the overall performance of SRL dominates RLib.

**5.1.3 Architecture Evaluation on Large-scale Cluster.** The worker-based abstraction and decoupled architecture design make SRL capable of running IMPALA-style and SEED-style architectures by simply setting different configurations. To evaluate the performance of different architectures in a large-scale cluster, we ran SRL in three different configurations: (1) fully decoupled actor, policy, and trainer workers; (2) decoupled actor workers with coupled trainer and policy workers (i.e., SEED-style); (3) coupled actor

Table 6: Computing resources in scalability experiments. AW: Actor Worker, PW: Policy Worker, TW: Trainer Worker. Each AW is allocated to one CPU core. 4 PWs are allocated to one GPU.

Env.	AW Per TW (Total) in Conf. 1&2	AW Per TW (Total) in Conf. 3	PW Per TW in Conf. 1
Atari	100 (3200)	400 (12800)	8
SMAC	160 (5120)	200 (6400)	4
gFootball	400 (12800)	400 (12800)	4
DMLab	200 (6400)	400 (12800)	8

and policy workers with trainer workers (i.e., IMPALA-style). To observe the impact of cluster size on SRL’s performance, we progressively increased the allocation of computing resources from a quarter of the cluster (8 A100 GPUs and 16 CPU nodes) to the entire cluster.

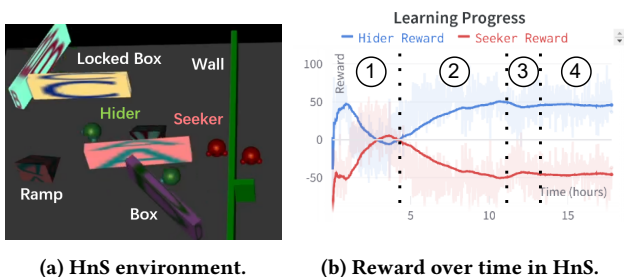
In order to strike a balance between maximizing performance and minimizing computing resource waste, we carefully determined the number of workers of each type and the allocated resources based on our ablation study (refer to Section 5.3). Table 6 presents the specific number of workers and computing resource utilization for each environment and architecture employed in this experiment.

Fig. 8 shows the full result of our experiments. As the computing resources increase, SRL exhibits proportional performance improvement across all architectures, indicating favorable scalability. In all four environments, Config 1, which is only available in SRL’s

architecture, effectively utilizes computing resources in the cluster and reach an optimal performance compared to other configurations. When employing a full-sized cluster, our novel architecture achieves a maximum FPS improvement of 3.74x compared to SEED-style architecture and 1.68x compared to IMPALA-style architecture. Only in environments where trainers could be easily overwhelmed by small numbers of actor workers (e.g. Atari) or GPU inference is less effective (e.g. SMAC), Config 3 (IMPALA-style) could reach the same performance as Config 1 by utilizing more CPU cores. To conclude, in the large-scale cluster, the architecture of SRL exhibit better resource efficiency than other architectures, leading to a significant performance improvement in all four environments.

## 5.2 Learning Performance

While quantifying the training throughput of SRL has yielded valuable insights into its efficiency and scalability, it is equally crucial to evaluate its ability to develop intelligent agents (i.e., learning performance) in a realistic and challenging environment. In this context, the hide-and-seek (HnS) environment [2] emerges as an appealing choice. Due to the complexity of this task, Baker et al. [2] employed the OpenAI Rapid system [5] for training, which makes it permissive for the research community to reproduce the results. In this section, we will demonstrate that SRL can not only replicate the findings reported in Baker et al. [2] with a remarkable 5x acceleration, but also effectively solve a more challenging variation of the HnS task using up to 15000 cores and 32 A100 GPUs. Such evaluations demonstrate the practical applicability of SRL and further shed light on its potential for addressing real-world problems.



**Figure 9: (a) A snapshot of HnS. (b) Rewards in HnS. Agent behavior evolves over four stages: running and chasing, box lock, ramp use, and ramp lock.**

**5.2.1 Problem Settings.** The hide-and-seek (HnS) environment [2] simulates a physical world which hosts 2-6 agents, including 1-3 hiders and 1-3 seekers, and diverse physical objects, including 3-9 boxes, 2 ramps, and randomly placed walls, as shown in Fig. 9a. Agents can manipulate boxes and ramps by moving or locking them, and locked objects can only be unlocked by teammates. At the beginning of each game, there is a preparation phase when seekers are not allowed to move, such that hiders can utilize available objects to build a shelter to defend seekers. After the preparation phase, seekers receive a reward +1 if any of them can discover hiders and -1 otherwise. Rewards received by hiders have opposite

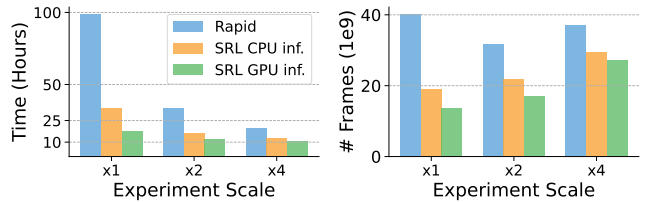


**Figure 10: Time/data required to reach stage four in HnS.**

signs. The observation, action, and additional environmental details can be found in Baker et al. [2].

Baker et al. [2] trains intelligent agents in HnS via PPO self-play with a complicated attention-based neural policy model. In particular, the same policy plays the roles of both hiders and seekers to collect data, and the RL algorithm merges these data together to update the policy. Through this approach, Baker et al. [2] discovered several stages of emergent behaviors across learning.

- (1) *Running and chasing.* Seekers learn to run and chase hiders while hiders simply run to escape seekers.
- (2) *Box lock.* Hiders build a shelter with locked boxes in the preparation phase to defend seekers.
- (3) *Ramp use.* Seekers learn to utilize ramps to jump over into the shelters built by hiders.
- (4) *Ramp lock.* Hiders first lock all ramps in the preparation phase and then build a shelter with locked boxes, such that seekers cannot move and utilize ramps.

The reward across this learning process is shown in Fig. 9b. Due to the non-trivial agent-object interactions and the complexity of the task, observing such behavior evolution requires an extremely large batch size, e.g. 320k interaction steps in a single batch. **We made our best efforts to run baseline systems in this environment, but none of them can handle training tasks in such a scale.**

We run SRL with the same environment configuration, policy model, and PPO hyper-parameters. Since Rapid is not open-source, nor the authors reveal how much computation resources they utilized, we are only able to compare with the reported numbers in the original paper (Fig. 4 in [2]).

**5.2.2 Computing Resources.** We conduct experiments in the distributed setting using both inline CPU inference (denoted as *CPU Inf.*) and remote GPU inference (denoted as *GPU Inf.*). We fixed the number of actor workers per trainer at 480 for *CPU Inf.*, each with a single environment, and 120 for *GPU Inf.*, each with an environment ring of size 20. *GPU Inf.* additionally uses 8 policy workers along with a trainer, which occupies two 3090 GPUs. We denote the smallest batch size 0.32M used in Baker et al. [2] as scale x1, which utilizes 4 trainer workers on A100 GPUs in our experiments. Experiments with larger scales duplicate all worker types and increase the batch size by a corresponding factor. Note that the largest scale in Baker et al. [2] is x4 while the largest scale in our experiments is x8.

**5.2.3 Results.** In our experiment, we present the training time and data volume required to achieve the ramp lock stage in HnS, as shown in Figure 10. Our results reveal that SRL is up to 3x faster than the Rapid system with the same architecture (*CPU Inf.*), while *GPU*

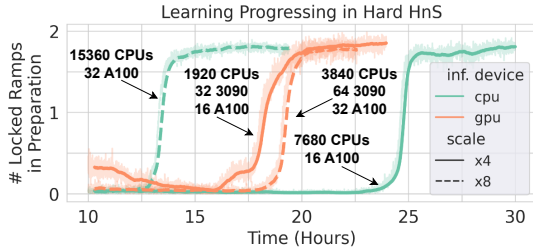


Figure 11: Learning progress in the hard setting of HnS.

*Inf.* can achieve up to 5x acceleration with further reduced time and environment interactions. We attribute the improvement in training efficiency to two reasons. First, our system design is more efficient and has a higher FPS than Rapid. Second, our flexible system design and fine-grained optimizations ensure that the efficiency of the RL algorithm is less affected by various system-related factors like network latency and out-of-date data, which leads to improved sample efficiency even with the same RL algorithm.

To explore the performance limit of SRL, we examine a more challenging HnS setting where we double the playground area’s size. This scenario has not been studied in previous works. Since the episode length is not changed, agents must learn to cooperatively search across a larger map for available objects and efficiently utilize the limited preparation phase. We run experiments with scale x4 and x8, and present learning progress over time in Fig. 11. With the same computation resources (i.e., x4), SRL requires almost twice the time to achieve the ramp lock stage in this new task, highlighting its difficulty. Interestingly, while *GPU Inf.* x8 attained similar performance compared to the x4 scale, *CPU Inf.* x8 halved the required training time. We remark that *CPU Inf.* x8 utilizes up to 15000+ CPU cores and 32 A100 GPUs, which is much beyond the computation used in most prior research papers. This outcome not only highlights the exceptional scalability of SRL, but also demonstrates the potential benefits of utilizing RL training, specifically PPO, at a larger scale.

### 5.3 Ablation Studies

This section presents a detailed analysis of the individual components of SRL. The purpose of these ablation studies is to offer practical recommendations for configuring SRL to achieve optimal performance in specific application scenarios. Our analysis encompasses fundamental systematic parameters and choices within SRL, such as the environment ring size, the employment of GPU inference and trainer worker pre-fetching, as well as the allocation of resources and ratios for each worker type. As shared-memory communication is typically faster than sockets, we assume its usage whenever possible and exclude the discussion of the communication backend in this section.

**5.3.1 Environment Ring.** Typically, environment ring size is the first thing that needs to be decided if GPUs are available and suitable for policy inference. This factor directly impacts the maximum rate at which a single actor worker can generate samples, thus playing a critical role in determining the optimal ratio between actor workers and other workers. We conduct an experiment to assess the effectiveness of the environment ring by measuring the

speed at which a single actor worker generates environment steps in different environments. To simulate situations of a practical experiment with optimized configuration, we use one GPU for inference, which is sufficient to minimize inference latency for a single actor worker. Fig. 12a illustrates how the speedup ratio varies with the size of the environment ring. As the ring size increases, the speedup ratio grows until it reaches a plateau. The experiment reveals that the ring size that reaches optimal performance differs across environments (around 16 for Atari, 10 for DMLab, 2 for Google Football and SMAC). Note that a larger ring size also means greater memory consumption by the actor worker. We believe that the optimal ring size is related to the average inference latency and the time it takes to execute a single environment step. The inference latency is similar across four environments, which suggests that the optimal ring size is determined by the step time. In this regard, Atari had the smallest step time, resulting in the largest optimal ring size and the highest speedup ratio of around 7x. Since in practical situations, inference latency could be influenced by various factors (e.g. network condition, GPU capabilities), it is the most reliable to find the optimal ring size for arbitrary environment by experiments that simulate the practical policy worker and actor worker setups. It is also a viable solution to estimate the theoretical optimal ring size by dividing average inference latency by environment step time.

**5.3.2 GPU inference vs CPU inference.** The next thing to determine is whether to use GPUs for policy inference and if so, how many GPUs should be used. From Fig. 8 we can see that if (1) the observation size is small, (2) the environment simulation speed is slow, and (3) the policy model is simple (e.g. a feed-forward network), inline CPU inference is usually sufficient. Otherwise, GPU inference can usually increase training throughput. If not GPUs are available for inference, increasing the number of actor workers is also a valid option. Figure 12d shows the results of our evaluation of the number of environment steps generated by 128 actor workers using different numbers of policy workers on GPU and inline inference on CPU. Both DMLab and Atari necessitate 2 GPUs for inference to achieve their optimal generation speed, resulting in a 1.56x and 5.44x speedup ratio, respectively. The difference between the two environments lies in the time taken for each environment step, with Atari taking less time than DMLab. Environments with a faster pace require increased computational power for inference within the same time period, resulting in a greater benefit from GPU inference acceleration. Google Football has a slower pace than DMLab and a simpler policy model due to its vector-based observation. Therefore, one GPU is sufficient for its inference. In contrast, SMAC is slower and has an even smaller-sized policy model. In such a scenario, inline inference with CPU performs almost as good as GPU inference.

**5.3.3 Maximizing Trainer Worker Throughput.** Once the environment ring size and the ratio between actor and policy workers are determined, the sample generation speed of the system is fixed. The next concern is to maximize the number of samples consumed by trainer workers while minimizing wasted training samples. In the subsequent analysis, we focus on scenarios with a single trainer worker, while the number of workers can be scaled proportionally

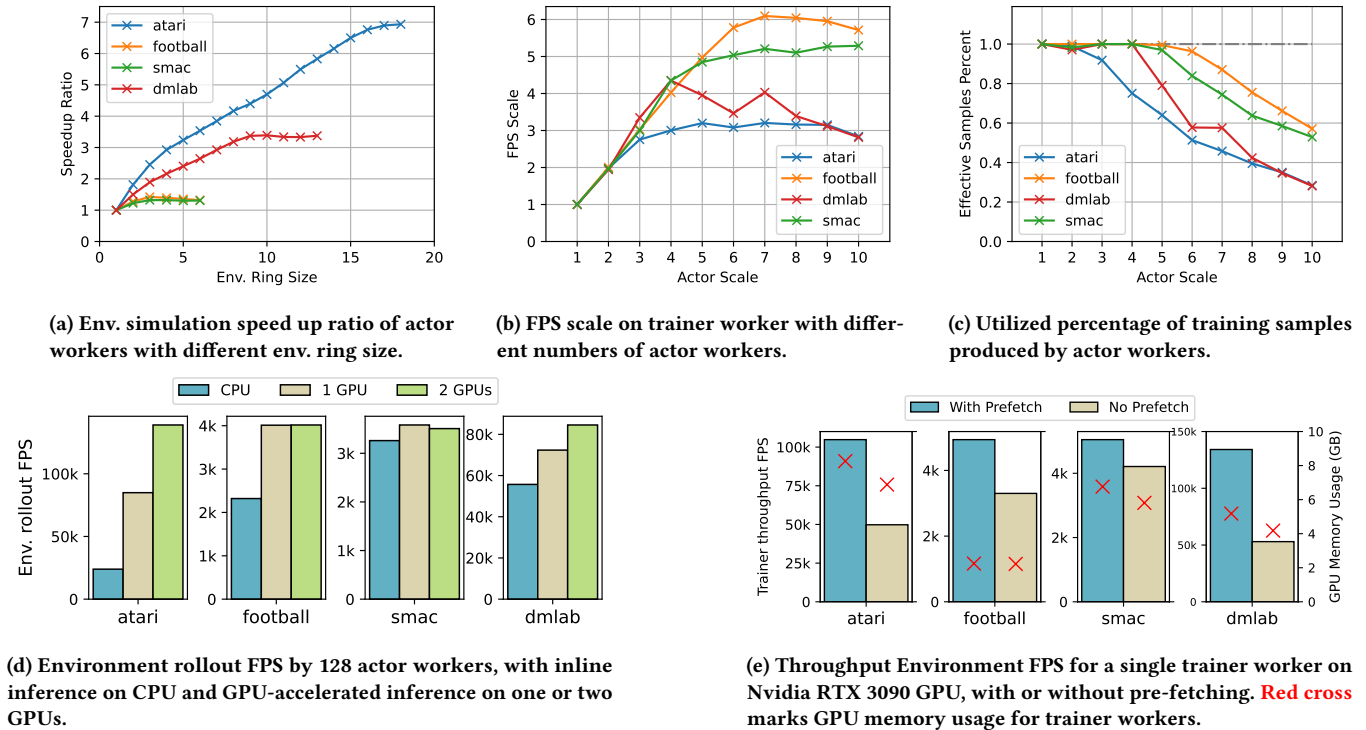


Figure 12: Ablation studies

for larger-scale experiments. To demonstrate the relationship between trainer frames-per-second (FPS) throughput and the number of actor workers, we assessed the training throughput of a single trainer consuming training samples generated by varying numbers of actor workers. Figure 12b illustrates that as the number of actors increases, the trainer FPS also rises until it reaches its maximum processing capacity. Beyond this point, the FPS experiences a slight decline due to network traffic congestion on the trainer worker. Notably, when a large number of actor workers are employed, redundant samples that cannot be utilized by the trainer are discarded. Figure 12c presents the utilization percentage of training samples generated by all actor workers on the trainer workers. When an excessive number of actor workers are allocated to a trainer worker, the utilization percentage sharply decreases with increasing actor workers, indicating a waste of training samples. It is important to note that the outcome in the DMLab environment exhibits instability as the number of actor workers increases. This is primarily due to the lengthy and highly variable reset time of the environment, which is inherent to the original environment implementation and lies beyond the scope of our system optimizations.

**5.3.4 Trainer Worker Pre-fetching.** In Section 4, we introduced the concept of pre-fetching in trainer workers, which involves a trade-off between GPU memory utilization and training speed. This technique can be employed whenever there is a sufficient amount of available GPU memory, which is commonly the case in reinforcement learning contexts. To demonstrate the effectiveness of pre-fetching, we conducted an experiment comparing the training

throughput and GPU memory utilization of a single trainer worker using an Nvidia 3090 GPU, both with and without the pre-fetching technique. The training batch size was fixed at 32. Our results, presented in Fig. 12e, indicate that utilizing pre-fetching can lead to a 2-3x increase in throughput for Atari and DMLab, but less speedup on Google Football and SMAC. We believe that this discrepancy is due to the fact that Atari and DMLab are image-based environments, which generates samples at a faster rate with a larger size, and possesses a more intricate policy model. Consequently, the trainer workers' capacity to consume samples and perform training operations can become a bottleneck. By increasing the number of samples that trainer workers can access through pre-fetching, the policy update process can be expedited, making it a more effective technique for such scenarios. On the other hand, GPU memory consumption are increased by 100 MBytes to 1.5 GBytes, which is bearable compared to total memory size (24 GBytes) of an Nvidia 3090 GPU.

## 6 RELATED WORKS

There have been several works aimed at developing systems and frameworks for training reinforcement learning agents [6, 7, 14, 15, 17, 21, 28, 30, 35, 36, 43, 44]. Some of these works solely focus on improving the sample throughput of training on a single machine. For instance, rlypt [35, 36] is a codebase that enables high-throughput RL training for small- to medium-scale researching scenarios. It supports parallel environment simulation and multi-GPU training on a single machine, and provides sampling options to optimize throughput in different scenarios. Subsequently, Sample Factory

[30] improved the single-machine throughput by optimizing shared-memory communications and resource efficiency techniques.

However, a single machine is typically insufficient to train strong RL agents. To address this limitation, OpenAI and DeepMind have developed large-scale distributed RL systems to train complex agents [5, 39]. Unfortunately, they never open-source their systems or explain the architecture or engineering details. The open-source versions [9] or community re-implementations [19] of these systems are typically limited to small-scale settings.

In addition to the aforementioned works, there have been open-source efforts to distribute RL training by proposing novel architectures and providing parallelized implementations. Some of these systems are designed for specific purposes. For example, Surreal [12] is an RL framework focused on robotic environments for continuous control, particularly MuJoCo [37]. On the other hand, ReAgent (also known as Horizon [14]) is an end-to-end platform designed for distributed recommendation or optimization tasks. While both Surreal and ReAgent support distributed execution, they may not be suitable for most RL algorithms and environments.

Regarding general-purpose distributed RL systems, RLLib [21] is a most popular one. It is an RL library implemented with Ray [27], a popular distributed framework for AI applications. RLLib supports parallel “actors” for stepping through the environment and generating data, and a single-node multi-GPU “learner”. Moreover, RLLib can utilize CPU resources across multiple machines to increase the speed of sample production. RLLib also offers a programming model called RLLib Flow [22] to reduce development efforts. It is worth noting that RLLib flow has been integrated into RLLib as its default interface, which we adopt in our experiments. ACME [17] is another open-source reinforcement learning framework that aims to scale up RL training. Its architecture and capabilities are similar to RLLib, but it is implemented with its own communication library, Launchpad [40]. Additionally, SeedRL [10] is an architecture that enables fast RL agent training on specialized TPU devices. It performs centralized policy inference and training on its single “learner” and can execute parallel environments across multiple machines. MSRL [44] is a concurrent work that aims to design a framework that unifies existing architectures. It transforms user-side RL training codes that runs on a local setting into “fragments” that executes in a distributed cluster following a pre-determined set of scheduling plans. The code from users should follow a restricted set of computation components and communication APIs and be marked by “annotations” as boundaries of fragments.

It is worth mentioning that there are also reinforcement learning libraries that serve as toolkits that allow users to develop their own RL training codes with less efforts. An example is TorchRL [26] as an extension of pytorch to support generating samples and implementing policy models. Moolib [24] is a RPC library that helps user to implement communication components in reinforcement training. Training an RL agent with these libraries requires users to implement their own training components, which means that their training performance will highly rely on user-end implementations.

## 7 CONCLUSION

This paper presents a novel abstraction on the dataflows of RL training. Based on the abstraction, we propose a scalable, efficient,

and extensible RL system. The novel abstraction and architecture of SRL enable massively parallelized computation and efficient resource allocation, and flexible worker scheduling, leading to high performance in both single machine and large scale scenarios. Also, the user-friendly and extensible interface of SRL facilitates customized environments, policies, and algorithms for users in SRL. Our experiment demonstrate the remarkable training throughput and learning performance of SRL across a wide range of application scenarios. In addition, through ablation studies, we provide helpful suggestions on designing an optimal configuration to maximize the performance of SRL.

## REFERENCES

- [1] Adrià Puigdomènech Badia, Bilal Piot, Steven Kapturovski, Pablo Sprechmann, Alex Vitvitskiy, Zhaohan Daniel Guo, and Charles Blundell. 2020. Agent57: Outperforming the atari human benchmark. In *International conference on machine learning*. PMLR, 507–517.
- [2] Bowen Baker, Ingmar Kanitscheider, Todor M. Markov, Yi Wu, Glenn Powell, Bob McGrew, and Igor Mordatch. 2019. Emergent Tool Use From Multi-Agent Autocurricula. *CoRR* abs/1909.07528 (2019). arXiv:1909.07528 <http://arxiv.org/abs/1909.07528>
- [3] Charles Beattie, Joel Z. Leibo, Denis Teplyashin, Tom Ward, Marcus Wainwright, Heinrich Küttler, Andrew LeFrancq, Simon Green, Víctor Valdés, Amir Sadik, Julian Schrittwieser, Keith Anderson, Sarah York, Max Cant, Adam Cain, Adrian Bolton, Stephen Gaffney, Helen King, Demis Hassabis, Shane Legg, and Stig Petersen. 2016. DeepMind Lab. *CoRR* abs/1612.03801 (2016). arXiv:1612.03801 <http://arxiv.org/abs/1612.03801>
- [4] Marc G. Bellemare, Yavar Naddaf, Joel Veness, and Michael Bowling. 2012. The Arcade Learning Environment: An Evaluation Platform for General Agents. *CoRR* abs/1207.4708 (2012). arXiv:1207.4708 <http://arxiv.org/abs/1207.4708>
- [5] Christopher Berner, Greg Brockman, Brooke Chan, Vicki Cheung, Przemyslaw Debiak, Christy Dennison, David Farhi, Quirin Fischer, Shariq Hashme, Christopher Hesse, Rafal Józefowicz, Scott Gray, Catherine Olsson, Jakub Pachocki, Michael Petrov, Henrique Pondé de Oliveira Pinto, Jonathan Raiman, Tim Salimans, Jeremy Schlatter, Jonas Schneider, Szymon Sidor, Ilya Sutskever, Jie Tang, Filip Wolski, and Susan Zhang. 2019. Dota 2 with Large Scale Deep Reinforcement Learning. *CoRR* abs/1912.06680 (2019). arXiv:1912.06680 <http://arxiv.org/abs/1912.06680>
- [6] Itai Caspi, Gal Leibovich, Gal Novik, and Shadi Endrawis. 2017. Reinforcement Learning Coach. <https://doi.org/10.5281/zenodo.1134899>
- [7] Pablo Samuel Castro, Subhodeep Moitra, Carles Gelada, Saurabh Kumar, and Marc G. Bellemare. 2018. Dopamine: A Research Framework for Deep Reinforcement Learning. *CoRR* abs/1812.06110 (2018). arXiv:1812.06110 <http://arxiv.org/abs/1812.06110>
- [8] Jonas Degraeve, Federico Felici, Jonas Buchli, Michael Neunert, Brendan Tracey, Francesco Carpanese, Timo Ewalds, Roland Hafner, Abbas Abdolmaleki, Diego de Las Casas, et al. 2022. Magnetic control of tokamak plasmas through deep reinforcement learning. *Nature* 602, 7897 (2022), 414–419.
- [9] Prafulla Dhariwal, Christopher Hesse, Oleg Klimov, Alex Nichol, Matthias Plappert, Alec Radford, John Schulman, Szymon Sidor, Yuhuai Wu, and Peter Zhokhov. 2017. OpenAI Baselines. <https://github.com/openai/baselines>.
- [10] Lasse Espeholt, Raphaël Marinier, Piotr Stanczyk, Ke Wang, and Marcin Michalski. 2019. SEED RL: Scalable and Efficient Deep-RL with Accelerated Central Inference. *CoRR* abs/1910.06591 (2019). arXiv:1910.06591 <http://arxiv.org/abs/1910.06591>
- [11] Lasse Espeholt, Hubert Soyer, Rémi Munos, Karen Simonyan, Volodymyr Mnih, Tom Ward, Yotam Doron, Vlad Firoiu, Tim Harley, Iain Dunning, Shane Legg, and Koray Kavukcuoglu. 2018. IMPALA: Scalable Distributed Deep-RL with Importance Weighted Actor-Learner Architectures. *CoRR* abs/1802.01561 (2018). arXiv:1802.01561 <http://arxiv.org/abs/1802.01561>
- [12] Linxi Fan, Yuke Zhu, Jiren Zhu, Zihua Liu, Orjen Zeng, Ankit Gupta, Joan Creus-Costa, Silvio Savarese, and Li Fei-Fei. 2018. SURREAL: Open-Source Reinforcement Learning Framework and Robot Manipulation Benchmark. In *Conference on Robot Learning*.
- [13] Alhussein Fawzi, Matej Balog, Aja Huang, Thomas Hubert, Bernardino Romera-Paredes, Mohammadamin Barekatain, Alexander Novikov, Francisco J R Ruiz, Julian Schrittwieser, Grzegorz Swirszcz, et al. 2022. Discovering faster matrix multiplication algorithms with reinforcement learning. *Nature* 610, 7930 (2022), 47–53.
- [14] Jason Gauci, Edoardo Conti, Yitao Liang, Kittipat Virochsiri, Yuchen He, Zachary Kaden, Vivek Narayanan, Xiaohui Ye, Zhengxing Chen, and Scott Fujimoto. 2018. Horizon: Facebook’s Open Source Applied Reinforcement Learning Platform. <https://doi.org/10.48550/ARXIV.1811.00260>

- [15] Danijar Hafner, James Davidson, and Vincent Vanhoucke. 2017. TensorFlow Agents: Efficient Batched Reinforcement Learning in TensorFlow. *CoRR* abs/1709.02878 (2017). arXiv:1709.02878 <http://arxiv.org/abs/1709.02878>
- [16] Kaiming He, Xiangyu Zhang, Shaoqing Ren, and Jian Sun. 2016. Deep Residual Learning for Image Recognition. In *2016 IEEE Conference on Computer Vision and Pattern Recognition, CVPR 2016, Las Vegas, NV, USA, June 27-30, 2016*. IEEE Computer Society, 770–778. <https://doi.org/10.1109/CVPR.2016.90>
- [17] Matt Hoffman, Bobak Shahriari, John Aslanides, Gabriel Barth-Maron, Feryal Behbahani, Tamara Norman, Abbas Abdolmaleki, Albin Cassirer, Fan Yang, Kate Baumli, Sarah Henderson, Alexander Novikov, Sergio Gómez Colmenarejo, Serkan Cabi, Çağlar Gülçehre, Tom Le Paine, Andrew Cowie, Ziyu Wang, Bilal Piot, and Nando de Freitas. 2020. Acme: A Research Framework for Distributed Reinforcement Learning. *CoRR* abs/2006.00979 (2020). arXiv:2006.00979 <https://arxiv.org/abs/2006.00979>
- [18] Karol Kurach, Anton Raichuk, Piotr Stanczyk, Michal Zajac, Olivier Bachem, Lasse Espeholt, Carlos Riquelme, Damien Vincent, Marcin Michalski, Olivier Bousquet, and Sylvain Gelly. 2019. Google Research Football: A Novel Reinforcement Learning Environment. *CoRR* abs/1907.11180 (2019). arXiv:1907.11180 <http://arxiv.org/abs/1907.11180>
- [19] Heinrich Küttler, Nantas Nardelli, Thibaut Lavril, Marco Selvatici, Viswanath Sivakumar, Tim Rocktäschel, and Edward Grefenstette. 2019. TorchBeast: A PyTorch Platform for Distributed RL. *CoRR* abs/1910.03552 (2019). arXiv:1910.03552 <http://arxiv.org/abs/1910.03552>
- [20] Shen Li, Yanli Zhao, Rohan Varma, Omkar Salpekar, Pieter Noordhuis, Teng Li, Adam Paszke, Jeff Smith, Brian Vaughan, Pritam Damania, and Soumith Chintala. 2020. PyTorch Distributed: Experiences on Accelerating Data Parallel Training. *CoRR* abs/2006.15704 (2020). arXiv:2006.15704 <https://arxiv.org/abs/2006.15704>
- [21] Eric Liang, Richard Liaw, Robert Nishihara, Philipp Moritz, Roy Fox, Joseph Gonzalez, Ken Goldberg, and Ion Stoica. 2017. Ray RLLib: A Composable and Scalable Reinforcement Learning Library. *CoRR* abs/1712.09381 (2017). arXiv:1712.09381 <http://arxiv.org/abs/1712.09381>
- [22] Eric Liang, Zhanghao Wu, Michael Luo, Sven Mika, and Ion Stoica. 2020. Distributed Reinforcement Learning is a Dataflow Problem. *CoRR* abs/2011.12719 (2020). arXiv:2011.12719 <https://arxiv.org/abs/2011.12719>
- [23] Siqi Liu, Guy Lever, Zhe Wang, Josh Merel, S. M. Ali Eslami, Daniel Hennes, Wojciech M. Czarnecki, Yuval Tassa, Shayegan Omidshafiei, Abbas Abdolmaleki, Noah Y. Siegel, Leonard Hasenclever, Luke Marris, Saran Tunyasuvunakool, H. Francis Song, Markus Wulfmeier, Paul Muller, Tuomas Haarnoja, Brendan D. Tracey, Karl Tuyls, Thore Graepel, and Nicolas Heess. 2022. From motor control to team play in simulated humanoid football. *Sci. Robotics* 7, 69 (2022). <https://doi.org/10.1126/scirobotics.abo0235>
- [24] Vegard Mella, Eric Hambro, Danielle Rothenmel, and Heinrich Küttler. 2022. moolib: A Platform for Distributed RL. (2022). <https://github.com/facebookresearch/moolib>
- [25] Volodymyr Mnih, Koray Kavukcuoglu, David Silver, Alex Graves, Ioannis Antonoglou, Daan Wierstra, and Martin A. Riedmiller. 2013. Playing Atari with Deep Reinforcement Learning. *CoRR* abs/1312.5602 (2013). arXiv:1312.5602 <http://arxiv.org/abs/1312.5602>
- [26] Vincent Moens. 2023. *TorchRL: an open-source Reinforcement Learning (RL) library for PyTorch*. <https://github.com/pytorch/rl>
- [27] Philipp Moritz, Robert Nishihara, Stephanie Wang, Alexey Tumanov, Richard Liaw, Eric Liang, William Paul, Michael I. Jordan, and Ion Stoica. 2017. Ray: A Distributed Framework for Emerging AI Applications. *CoRR* abs/1712.05889 (2017). arXiv:1712.05889 <http://arxiv.org/abs/1712.05889>
- [28] Fabio Pardo. 2020. Tonic: A Deep Reinforcement Learning Library for Fast Prototyping and Benchmarking. *CoRR* abs/2011.07537 (2020). arXiv:2011.07537 <https://arxiv.org/abs/2011.07537>
- [29] Julien Pérolat, Bart De Vylder, Daniel Hennes, Eugene Tarassov, Florian Strub, Vincent de Boer, Paul Muller, Jerome T. Connor, Neil Burch, Thomas W. Anthony, Stephen McAleer, Romuald Elie, Sarah H. Cen, Zhe Wang, Audrunas Gruslys, Aleksandra Malysheva, Mina Khan, Sherjil Ozair, Finbarr Timbers, Toby Pohlen, Tom Eccles, Mark Rowland, Marc Lanctot, Jean-Baptiste Lespiau, Bilal Piot, Shayegan Omidshafiei, Edward Lockhart, Laurent Sifre, Nathalie Beauguerlange, Rémi Munos, David Silver, Satinder Singh, Demis Hassabis, and Karl Tuyls. 2022. Mastering the Game of Stratego with Model-Free Multiagent Reinforcement Learning. *CoRR* abs/2206.15378 (2022). <https://doi.org/10.48550/arXiv.2206.15378>
- [30] Aleksei Petrenko, Zhehui Huang, Tushar Kumar, Gaurav S. Sukhatme, and Vladlen Koltun. 2020. Sample Factory: Egocentric 3D Control from Pixels at 10000 FPS with Asynchronous Reinforcement Learning. *CoRR* abs/2006.11751 (2020). arXiv:2006.11751 <https://arxiv.org/abs/2006.11751>
- [31] Mikayel Samvelyan, Tabish Rashid, Christian Schroeder de Witt, Gregory Farquhar, Nantas Nardelli, Tim G. J. Rudner, Chia-Man Hung, Philip H. S. Torr, Jakob Foerster, and Shimon Whiteson. 2019. The StarCraft Multi-Agent Challenge. *CoRR* abs/1902.04043 (2019).
- [32] Julian Schrittwieser, Ioannis Antonoglou, Thomas Hubert, Karen Simonyan, Laurent Sifre, Simon Schmitt, Arthur Guez, Edward Lockhart, Demis Hassabis, Thore Graepel, Timothy P. Lillicrap, and David Silver. 2019. Mastering Atari, Go, Chess and Shogi by Planning with a Learned Model. *CoRR* abs/1911.08265 (2019). arXiv:1911.08265 <http://arxiv.org/abs/1911.08265>
- [33] John Schulman, Filip Wolski, Prafulla Dhariwal, Alec Radford, and Oleg Klimov. 2017. Proximal Policy Optimization Algorithms. *CoRR* abs/1707.06347 (2017). arXiv:1707.06347 <http://arxiv.org/abs/1707.06347>
- [34] David Silver, Aja Huang, Chris J. Maddison, Arthur Guez, Laurent Sifre, George van den Driessche, Julian Schrittwieser, Ioannis Antonoglou, Veda Panneershelvam, Marc Lanctot, Sander Dieleman, Dominik Grewe, John Nham, Nal Kalchbrenner, Ilya Sutskever, Timothy Lillicrap, Madeleine Leach, Koray Kavukcuoglu, Thore Graepel, and Demis Hassabis. 2016. Mastering the Game of Go with Deep Neural Networks and Tree Search. *Nature* 529, 7587 (jan 2016), 484–489. <https://doi.org/10.1038/nature16961>
- [35] Adam Stooke and Pieter Abbeel. 2018. Accelerated Methods for Deep Reinforcement Learning. *CoRR* abs/1803.02811 (2018). arXiv:1803.02811 <http://arxiv.org/abs/1803.02811>
- [36] Adam Stooke and Pieter Abbeel. 2019. rlpyt: A Research Code Base for Deep Reinforcement Learning in PyTorch. *CoRR* abs/1909.01500 (2019). arXiv:1909.01500 <http://arxiv.org/abs/1909.01500>
- [37] Emanuel Todorov, Tom Erez, and Yuval Tassa. 2012. MuJoCo: A physics engine for model-based control. In *2012 IEEE/RSJ International Conference on Intelligent Robots and Systems, IROS 2012, Vilamoura, Algarve, Portugal, October 7-12, 2012*. IEEE, 5026–5033. <https://doi.org/10.1109/IROS.2012.6386109>
- [38] Ashish Vaswani, Noam Shazeer, Niki Parmar, Jakob Uszkoreit, Llion Jones, Aidan N. Gomez, Lukasz Kaiser, and Illia Polosukhin. 2017. Attention is All you Need. In *Advances in Neural Information Processing Systems 30: Annual Conference on Neural Information Processing Systems 2017, December 4-9, 2017, Long Beach, CA, USA*, Isabelle Guyon, Ulrike von Luxburg, Samy Bengio, Hanna M. Wallach, Rob Fergus, S. V. N. Vishwanathan, and Roman Garnett (Eds.), 5998–6008. <https://proceedings.neurips.cc/paper/2017/hash/3f5ee243547dee91fbd053c1c4a845aa-Abstract.html>
- [39] Oriol Vinyals, Igor Babuschkin, Wojciech M. Czarnecki, Michaël Mathieu, Andrew Dudzik, Junyoung Chung, David H. Choi, Richard Powell, Timo Ewalds, Petko Georgiev, Junhyuk Oh, Dan Horgan, Manuel Kroiss, Ivo Danihelka, Aja Huang, Laurent Sifre, Trevor Cai, John P. Agapiou, Max Jaderberg, Alexander S. Vezhnevets, Rémi Leblond, Tobias Pohlen, Valentin Dalibard, David Budden, Yury Sulsky, James Molloy, Tom L. Paine, Caglar Gulcehre, Ziyu Wang, Tobias Pfaff, Yuhuai Wu, Roman Ring, Dani Yogatama, Dario Wunsch, Katrina McKinney, Oliver Smith, Tom Schaul, Timothy Lillicrap, Koray Kavukcuoglu, Demis Hassabis, Chris Apps, and David Silver. 2019. Grandmaster level in StarCraft II using multi-agent reinforcement learning. *Nature* 575, 7782 (01 Nov 2019), 350–354. <https://doi.org/10.1038/s41586-019-1724-z>
- [40] Fan Yang, Gabriel Barth-Maron, Piotr Stańczyk, Matthew Hoffman, Siqi Liu, Manuel Kroiss, Aedan Pope, and Alban Rustemi. 2021. Launchpad: A Programming Model for Distributed Machine Learning Research. *arXiv preprint arXiv:2106.04516* (2021). <https://arxiv.org/abs/2106.04516>
- [41] Deheng Ye, Guibin Chen, Wen Zhang, Sheng Chen, Bo Yuan, Bo Liu, Jia Chen, Zhao Liu, Fuhao Qiu, Hongsheng Yu, Yinyuting Yin, Bei Shi, Liang Wang, Tengfei Shi, Qiang Fu, Wei Yang, Lanxiao Huang, and Wei Liu. 2020. Towards Playing Full MOBA Games with Deep Reinforcement Learning. In *Advances in Neural Information Processing Systems 2020, NeurIPS 2020, December 6-12, 2020, virtual*, Hugo Larochelle, Marc’Aurelio Ranzato, Raia Hadsell, Maria-Florina Balcan, and Hsuan-Tien Lin (Eds.). <https://proceedings.neurips.cc/paper/2020/hash/06d5ae105ea1bea4d800bc96491876e9-Abstract.html>
- [42] Andy B. Yoo, Morris A. Jette, and Mark Grondona. 2003. SLURM: Simple Linux Utility for Resource Management. In *Job Scheduling Strategies for Parallel Processing*, Dror Feitelson, Larry Rudolph, and Uwe Schwiegelshohn (Eds.). Springer Berlin Heidelberg, Berlin, Heidelberg, 44–60.
- [43] Jiale Zhi, Rui Wang, Jeff Clune, and Kenneth O. Stanley. 2020. Fiber: A Platform for Efficient Development and Distributed Training for Reinforcement Learning and Population-Based Methods. *CoRR* abs/2003.11164 (2020). arXiv:2003.11164 <https://arxiv.org/abs/2003.11164>
- [44] Huanzhou Zhu, Bo Zhao, Gang Chen, Weifeng Chen, Yijie Chen, Liang Shi, Yaodong Yang, Peter Pietzuch, and Lei Chen. 2022. MSRL: Distributed Reinforcement Learning with Dataflow Fragments. arXiv:2210.00882 [cs.LG]